Multichannel Silicon Probes for Awake Hippocampal Recordings in Large Animals

Alexandra V. Ulyanova[1], Carlo Cottone[1], Christopher D. Adam[1], Kimberly G. Gagnon[1], D. Kacy Cullen[1,4], Tahl Holtzmann[2], Brian Jameison[3], Paul F. Koch[1], H. Isaac Chen[1,4], Victoria E. Johnson[1], and John A. Wolf[1,4] *

[1] Center for Brain Injury and Repair, Department of Neurosurgery, Perelman Medical School, University of Pennsylvania;
[2] Cambridge NeuroTech;
[3] Scientific & Biomedical Microsystems
[4] Corporal Michael J. Crescenz Veterans Affairs Medical Center;
* Correspondence: wolfjo@pennmedicine.upenn.edu; Tel.: +1-215-746-4680

Abstract

Decoding laminar information across deep brain structures and cortical regions is necessary in order to understand the spatiotemporal ensembles that represent cognition and memory. Large animal models are essential for translational research due to their gyrencephalic neuroanatomy and significant white matter composition. One of the major obstacles to applying the approaches currently utilized in lower order animals are technical limitations in silicon probes, specifically a lack of long-length probes with appropriate stiffness to penetrate to deeper structures with minimal damage to the neural interface. We tested various solutions and designs of multichannel silicon probes developed for large animal electrophysiology by recording neurophysiological signals from deep laminar structures in an acute preparation and in chronically implanted awake behaving Yucatan pigs. Electrophysiological parameters of single units and local field potentials were analyzed to evaluate performance over time of given silicon probes in chronic implantations. The cross-sectional area of silicon probes was found to be a crucial determinant of silicon probes' single unit performance over time, potentially due to reduction of damage to the neural interface. EDGE-style probes had the highest yields during intra-hippocampal recordings in pigs, making them the most suitable for chronic implantations and awake behavioral experimentation. Novel CAMB 64-channel EDGE-style probes with linear and poly-2 site arrangement tested acutely had optimal single unit separation and a denser sampling of the laminar structure, identifying them as potential candidates for chronic implantations with less cortical damage above the active portion of the probe. This study provides an analysis of multichannel silicon probes designed for large animal laminar electrophysiology of deep brain structures, and suggests that current designs are reaching the physical thresholds necessary for long-term (~ 1 month) recordings from laminar deep structures with single-unit resolution.

Keywords: large animals, pigs, multichannel silicon probes, laminar hippocampal electrophysiology, awake chronic recordings

Introduction

Spatio-temporal neuronal ensembles distributed throughout laminar structures in the brain such as the cortex and hippocampus are presumed to be the substrate for cognition and memory. Oscillatory activity and resulting power bands are transmitted throughout the layers of laminar structures as different inputs are driven at different frequencies depending on their area of origin [1-5]. Laminar analyses of oscillatory activity have proven valuable for elucidating circuit dynamics as well as changes between states in both cortex and hippocampus [5, 6]. Traditionally, single neurons have been analyzed independently on the basis of their tuning to sensory stimuli or movement. Although tuning curve approaches are unaffected by growing numbers of simultaneously recorded neurons, newly developed techniques that analyze interactions between neurons become more complex as the number of recorded neurons increases [7]. For spike-field entrainment analyses, it is also important to know where inputs that drive the cells originate and how they interact locally. Cell types, dendritic arborization, local and long-range axonal projections all distribute unevenly across layers, shaping the integration and segregation of neural signals. Ultimately, we must decode laminar information across different structures to understand the spatiotemporal ensembles that represent cognition and memory. Thus, measuring the coordination of spiking activity of large numbers of neurons, and specifically those thought to give rise to distributed functional networks, is critical for understanding neural information processing underlying cognition and behavior [6].

The hippocampus is an example of a deep laminar structure that is highly involved in encoding episodic memory formation presumably via spatiotemporal ensembles of neurons. Once multichannel silicon probes were developed, they quickly became a standard tool for awake hippocampal neurophysiological recordings in rodents [8] . Increasing the density of laminar contacts in deep structures allows researchers to gain more information about these structures and more recently, study the potential effects of neurological disease states on single unit activity [9-11]. Recent advances in high-density linear electrode arrays and wireless recording technology could tremendously enhance studies of large-scale networks in species with large, gyrencephalic brains. Although the rodent hippocampus has been studied in great detail, the transition to large animal models has been slower. One of the major obstacles to addressing the research questions and approaches currently accessible in rodents are technical limitations in laminar silicon microelectrodes. Much of the large animal brain is still inaccessible due to insufficient length of available silicon probes. In large animals and humans, the hippocampus is located sub-cortically is therefore difficult to study electrophysiologically using multi-channel probes. Even many cortical targets cannot be reached with the current technology including those typically utilized for brain machine interface (BMIs) such at the Utah electrode. In addition, laminar structure cannot be detected with single wire or tetrode recordings. Existing non-laminar solutions can scale to high density, but have single contacts at the tip, limiting the ability to differentiate single units or

localize them within the laminar circuitry [12]. Therefore, current technology is not suitable for understanding within and between laminar structures.

Ideally, the probes for electrophysiological recordings from deep brain structures must resolve laminar local field potentials (LFPs) and provide proper sampling densities to resolve single-units across channels for single unit spike-sorting. For instance, multi-channel silicon probes with many contacts in a linear configuration can isolate units in a 2-300 μm "sphere" around each electrode [13, 14]. Layer-specific fields can convey information transmitted from other regions, while direct, local spiking activity can be measured simultaneously. Silicon probes also need to be long enough to reach these structures, while remaining narrow and flexible to match brain tissue properties and to tissue damage. Multiple inserted probes could also provide highly detailed information about local and long-range circuit computations in multiple regions with little damage to the neural interface using these new technologies if the right balance between these factors could be resolved [6].

Technology necessary to produce finer features at longer length has only recently became available, including stitching across the dye in the photomask process to utilize smaller feature processes. New multichannel silicon probes designed for large animal electrophysiology allow for simultaneous recordings of fields and spikes from multiple layers of laminar structures such as cortex and hippocampus, and we therefore tested various designs of laminar silicon probes suitable for large animals. Across probe designs, we compared neurophysiological characteristics and biomechanical compatibility with effects on insertion ability based on the variables such as probe thickness and site arrangement. Current technology in silicon probes appears to have reached the critical size/feature dimension where units can be obtained for chronic periods in deep structures without extensive damage to the neural interface, while still maintaining insertion stiffness. Further refinement of these probe technologies in combination with chronic drives and wireless technology may usher in a new high-density era for previously unexplored regions of cortex, hippocampus and other non-laminar deep structures in large animals and potentially humans.

Materials and Methods

Animals

Male Yucatan miniature pigs, which were chosen for their docile temperament, ease of handling, and slow growth rate for future chronic studies were used in this study. Pigs were purchased from Sinclair and underwent the current studies at the approximate age of 5 - 6 months at a mean weight of 38 ± 3 kg (n = 17, mean ± SEM). We chose this age because the pigs are post-adolescent with near-fully developed brains, and young enough to be of a manageable weight for procedures and behavior [15-17]. All pigs were pair housed when possible, and were always in a shared room with other pigs. All animal procedures were performed in accordance with the University of Pennsylvania animal care committee's regulations, an AALAC accredited institution.

Surgical Procedure

Yucatan miniature pigs (NSRRC, Catalog # 0012, RRID: NSRRC_0012) were fasted for 16 hours then induced with 20 mg/kg of ketamine and 0.5 mg/kg of midazolam. Animals were intubated with an endotracheal tube and anesthesia was maintained with 2-2.5% isoflurane per 2 liters O_2. Each animal was placed on a ventilator and supplied oxygen at a tidal volume of 10 mL/kg. A catheter was placed in an auricular vein to deliver 0.9% normal saline at 200 mL per hour. Additionally, heart rate, respiratory rate, arterial oxygen saturation, end tidal CO_2 and rectal temperature were continuously monitored, while pain response to pinch was periodically assessed. All of these measures were used to titrate ventilation settings and isoflurane percentage to maintain an adequate level of anesthesia. A forced air warming system was used to maintain normothermia throughout the procedure.

All chronically implanted animals in this study underwent implantation of multi-channel silicon probe under sterile conditions similar to acute implantation procedure described previously [18]. Briefly, pigs were placed in a stereotactic frame, with the surgical field prepped and draped, and a linear incision was made along the midline. A 13-mm diameter burr hole was centered at 7 mm lateral to the midline and 4.5 mm posterior to bregma, and the bony opening was subsequently expanded using Kerrison punches. Skull screws were placed over the occipital ipsilateral and contralateral cortex as a ground and alternate reference signal. The dura was opened in a cruciate manner and the dorsal hippocampus was first mapped with a tungsten electrode (impedance = 0.5 MΩ) in the sagittal plane, utilizing observed spiking activity to generate a two-dimensional map. Based on this map, the coordinates for insertion of multichannel silicon probes were then chosen such that the spread of electrode contacts would span the laminar structure of the dorsal hippocampus at its maximal thickness in the dorsal-ventral plane, perpendicular to the individual hippocampal layers. The silicon probe was inserted and neurophysiological signals were tested under anesthesia to ensure signal quality and placement along the dorso-ventral axis using LFP features. The multichannel silicon probe was stabilized inside the craniectomy using Tisseel (Baxter Healthcare, Catalog # 1504514), creating a semi-floating interface between the silicon probe and the animal's skull. The probe cables were fed through the head cap chamber and attached to a custom electrode interface board (EIB) adapter. The head cap chamber, which covered silicon probe and all necessary electronic connections, was attached to the pig skull using anchor screws and secured with bone cement and geristore. Once the quality of signals from multichannel silicon depth probes were confirmed, hippocampal signals were first recorded under anesthesia using a QC-72 amplifier and referenced to both internal and skull references. This recording was later used as a baseline for awake recordings and to monitor silicon probe's position over time for possible drift.

Multichannel Silicon Probes

32-channel silicon probes designed for large animal electrophysiology were designed with ATLAS Neuroengineering (ATLAS32/TET, Catalog # E32T7-R-275-S01-L25) and NeuroNexus (VECTOR style probes: NN32/EDGE150 and NN32/EDGE80 (Catalog # V1x32-Edge-10mm-200-312-Ref) and NN32/TET (Custom design, Catalog # V1x32-

80mm-275-tet-177-HP32). In addition, 64-channel silicon research probes were developed in a collaboration with SBM (Scientific & Biomedical Microsystems) and Cambridge NeuroTech. These silicon probes were tested acutely for comparative purposes and to improve future outcome for chronic implantation of silicon probes. These 64-channel silicon probes had either a linear (CAMB64/LIN) or poly-2 (CAMB64/POLY-2) style arrangement of the individual electrode sites. The arrangement of the individual electrode site/channels for all probes listed above is shown in Figure 1 (see below). All multichannel silicon probes were designed with one low-impedance channel placed 1-2 mm above adjacent proximal channel, which was used as an internal reference. For dorsal hippocampal targeting, this design provides 31 (or 63) channels for intra-hippocampal recordings with the reference channel being positioned within the temporal horn of the lateral ventricle dorsal to the hippocampus.

Neural Data Collection and Analysis

Electrophysiological recordings with 32-channel silicon probes (ATLAS32/TET, NN32/TET, NN32/EDGE150, and NN32/EDGE80) were performed in awake behaving animals at various time points at up to 6 months post implantation. Wide bandwidth neural signals were acquired continuously, sampled at 30 kHz with FreeLynx digital acquisition system, amplified and either wirelessly transmitted to Digital Lynx 4SX acquisition system with Cheetah recording and acquisition software during behavioral space recordings or stored to on-board MicroSD memory during home cage recordings (Neuralynx, Inc.). Recordings with 64-channel silicon probes (CAMB64/LIN and CAMB64/POLY-2) were performed acutely under anesthesia, with wide band neural signals continuously acquired, sampled at 32 kHz and amplified with Digital Lynx 4SX acquisition system with Cheetah recording and acquisition software (Neuralynx, Inc.).

Spike Detection and Analysis: Neural signals acquired from the 31 and/or 63 channels on the silicon probes were bandpass filtered (0.1 Hz to 9 kHz) in real time prior to sampling. Off-line spike detection and sorting was performed on the wideband signals using the Klusta package (http://klusta-team.github.io/klustakwik/, RRID: SCR_014480), which was developed for higher density electrodes, and manually refined with KlustaViewa or Phy (https://github.com/klusta-team/klustaviewa). The Klusta packages are designed to construct putative clusters from all probe channels simultaneously by taking advantage of spike timing and the special arrangement of electrode sites [19]. After manual refinement, resulting single-unit clusters were then imported into Matlab software, version R2017a for visualization and further analysis using custom and built-in routines (https://www.mathworks.com/products/matlab.html, RRID: SCR_001622).

Analysis of Local Field Potentials (LFPs): Acquired wideband LFPs recorded from all channels of the silicon probe were down-sampled to 2 kHz for further analysis. Signals were imported into Matlab software, version R2017a (https://www.mathworks.com/products/matlab.html, RRID: SCR_001622) and processed using a combination of custom and modified scripts from the freely available Matlab

packages FMAToolbox (http://fmatoolbox.sourceforge.net, RRID: SCR_015533), Chronux (http://chronux.org, RRID: SCR_005547), and EEGLAB (http://sccn.ucsd.edu/eeglab/index.html, RRID: SCR_007292) [20, 21].

Tissue Handling and Histological Examinations

Histological analyses were performed to identify electrode tracks on brain tissue from male Yucatan miniature pigs. At the study endpoint, under anesthesia transcardial perfusion was performed using 0.9% heparinized saline followed by 10% neutral buffered formalin (NBF). After further post-fixation for 7 days in 10% NBF at 4°C, the brain was dissected into 5 mm blocks in the coronal plane and processed to paraffin using standard techniques [22, 23]. 8 µm sections were obtained at the level of the hippocampus in and standard hematoxylin & eosin (H&E) staining was performed on all animals to identify electrode tracks. The following additional stains were performed:

Van Gieson's Staining: Tissue sections were dewaxed in xylenes and rehydrated to water via graded ethanols before being immersed in Weigert's Working Hematoxylin solution, prepared by mixing equal parts of Weigert's Iron Hematoxylin A (EMS, Catalog # 26044-05) and Weigert's Iron Hematoxylin B (EMS, Catalog # 26044-15) for 10 minutes. After rinsing in distilled water, tissue sections were stained for 3 minutes in Van Gieson's solution (EMS, Catalog # 26046-05). After further rinsing, slides were differentiated in 95% ethanol with 0.001% acetic acid, dehydrated, cleared in xylenes and coverlipped.

Immunohistochemistry (IHC): IHC labeling was performed according to previously published protocols [24-26]. Briefly, tissue sections were dewaxed and rehydrated as above, followed by immersion in 3% aqueous hydrogen peroxide for 15 minutes to quench endogenous peroxidase activity. Antigen retrieval was achieved via microwave pressure cooker at high power for 8 minutes, submerged in Tris EDTA buffer (pH 8.0). Sections were then incubated overnight at 4°C using antibodies specific for the N-terminal amino acids 66–81 of the amyloid precursor protein (APP) (Millipore, Burlington MA, clone 22C11 at 1:80K), GFAP (Leica, Biosystems, Buffalo Grove, IL, GA5 clone at 1:10K, and IBA1 (Wako Chemicals USA Inc. Richmond, VA at 1:7K). Slides were then rinsed and incubated in the relevant species-specific biotinylated universal secondary antibody for 30 minutes at room temperature. Next, application of the avidin biotin complex (Vector Laboratories, Catalog # PK-6200, Lot # RRID: AB_2336826) was performed for 30 minutes, also at room temperature. Lastly, the 3, 3'-diaminobenzidine (DAB) peroxidase substrate kit (Vector Laboratories, Catalog # SK-4100, Lot # RRID: AB_233638) was applied according to manufacturer's instructions. All sections were counterstained with hematoxylin, dehydrated in graded ethanols, cleared in xylenes, and cover slipped.

Statistical Analysis

The data was analyzed using Graphpad Prism software, version 7 (http://www.graphpad.com/, PRID: SCR_002798). Single unit waveforms recorded with silicon laminar probes are displayed as mean ± SD. Amplitudes of single units are displayed as mean ± SEM. Impedance of silicon probes is shown as mean ± SEM.

Results

Neurophysiological signals were recorded from the dorsal hippocampus of miniature Yucatan pigs with custom-designed laminar silicon probes. Performance of multi-channel silicon probes were first examined during surgery (acutely) and then over time post implantation (months). Various silicon probes were evaluated for their ability to continuously record laminar oscillatory and single unit activity in awake behaving pigs and for neuropathological changes induced by their placement in the porcine hippocampus over time. In order to improve outcome of future chronic implantations, novel 64-channel silicon probes were custom-designed to have a reduced cross-sectional area and using a full-length silicon design rather than a silicon plus tube design. Mock versions of these 64-channel probes were first tested for their insertion ability during acute testing. The thinnest version of the 64-channel silicon probe that was capable of insertion was later evaluated for its ability to detect and sort single vs. multi-unit activity using two electrode geometries.

Silicon Probe	**Layout**	**Spacing (μm)**	**Area (μm^2)**	**Imp (MΩ)**	**Electrode Material**	**Thickness (μm)**	**Width (μm)**	**Area (μm^2)**
ATLAS32/ TET	tetrode[1] + linear	275[2]	962	1.29	Pt	100	215	21,500
NN32/ TET	tetrode[1] + linear	275[2]	312	1.68	IrOx	50	225	11,250
NN32/ EDGE150	edge[3]	200	312	1.81	IrOx	50	150	7,500
NN32/ EDGE80	edge[3]	200	312	1.81	IrOx	50	80	4,000
CAMB64/ LIN	linear + edge[3]	100	165	0.06	Au	35	148	5,180
CAMB64/ POLY-2	poly-2[4] + edge[3]	100	165	0.06	Au	35	154	5,390

Table 1. Multi-channel silicon probes for chronic hippocampal recordings in pigs.

[1] an arrangement of four electrode sites placed close together;

[2] spacing between individual tetrodes (at first site) as well as between linear sites;

[3] similar to the linear layout, but electrode sites are positioned at the edge of the substrate;

[4] similar to the linear layout, but electrode sites are off-set by 21 μm relative to each other.

Design of Silicon Probes for Large Animal Chronic Implantations

Multichannel silicon probes were designed to have either 32 or 64 electrode sites arranged in various configurations (Figure 1). To maximize spike sorting while using an earlier version of the spike sorting software, some silicone probes (ATLAS32/TET and NN32/TET) were designed to have a tetrode arrangement of the electrode sites. To resolve laminar structure of the porcine hippocampus and to maximize spike sorting while using the latest spike sorting software, additional silicone probes were designed to have either a linear (CAMB64/LIN, NN32/EDGE150, and NN32/EDGE80) or a poly-2 (CAMB64/POLY-2) arrangement of the electrode sites. For dorsal hippocampal targeting in pigs, these designs provide 31 (or 63) channels for laminar recordings and results in the reference channel being positioned within the temporal horn of the lateral ventricle sitting just above the hippocampus (not shown). Specific parameters of multichannel silicon probes tested in this study are summarized in Table 1. The detailed description of multichannel silicon probes designed for pig hippocampal recordings in chronically as well as acutely implanted pigs are listed in Table 1.

ATLAS32/TET: 32-channel silicon probes have a custom design individual sites arranged in groups of four closely spaced sites or tetrodes (Figure 1A). During chronic hippocampal recordings, the top four tetrodes were placed in pyramidal CA1 layer, while the bottom three tetrodes were placed in granular cell layer. Three linear sites in between groups of tetrodes were added to cover pig hippocampal layers of strata radiatum, lacunosum-moleculare and moleculare. The top site on each tetrode along with linear sites were placed 275 μm to form 10 equally spaced sites for laminar hippocampal recordings. The total cross-sectional area of the individual electrode site was 21,500 μm^2 (Figure 1B). The total coverage of ATLAS32/TET recording sites was set to 2750 μm. The individual electrode sites had a diameter of 35 μm and were coated with Pt [27]. The averaged impedance was 1.29 ± 0.21 MΩ (mean ± SEM, $n_{probes} = 5$).

NN32/TET: 32-channel silicon probes have a custom design individual sites arranged in groups of four closely spaced sites or tetrodes (Figure 1A). During chronic hippocampal recordings, the top four tetrodes were placed in pyramidal CA1 layer, while the bottom three tetrodes were placed in granular cell layer. Three linear sites in between groups of tetrodes were added to cover pig hippocampal layers of strata radiatum, lacunosum-moleculare and moleculare. The top site on each tetrode along with linear sites were placed 275 μm to form 10 equally spaced sites for laminar hippocampal recordings. The total cross-sectional area of the individual electrode site was 11,250 μm^2 (Figure 1B). The total coverage of NN32/TET recording sites was set to 2750 μm. The individual electrode sites on NN32/TET silicon probes were coated with IrOx and had an impedance of 1.68 ± 0.20 MΩ (mean ± SEM, $n_{probes} = 13$).

NN32/EDGE150 and NN32/EDGE80: 32-channel silicon probes have a linear site arrangement, with 200 μm site spacing. The individual sites were strategically positioned at the edge of the substrate (Figure 1A). The total cross-sectional area of the individual electrode site was 7,500 μm^2 for NN32/EDGE150 and 4,000 μm^2 for NN32/EDGE80 silicon probes (Figure 1B). The total coverage of NN32/EDGE150 and NN32/EDGE80 recording sites was

6200 μm. These silicon probes also had an internal reference (surface area = 1400 μm^2) placed 1.5 mm above the most-proximal site of the probe (not shown). The individual electrode sites are coated with IrOx and have an impedance of 1.68 ± 0.20 MΩ (mean ± SEM, n_{probes} = 13).

CAMB64/LIN: Acutely tested 64-channel silicon probes have 63 individual channels arranged linearly at the edge of the probe with 100 μm site spacing (Figure 1A, also see insert). The top most channel was substituted for an internal reference with surface area = 1404 μm^2 and placed 1.75 mm above the most-proximal site of the probe (not shown). The total cross-sectional area of the individual electrode site was 5,180 μm^2 (Figure 1B). The total coverage of recording electrode sites was 6300 μm. The individual electrode sites were coated with Au and had an impedance of 0.063 ± 0.001 MΩ (mean ± SEM, n_{sites} = 63; n_{probes} = 1). Smaller feature of CAMB64/LIN silicon probes was achieved with a process of high-resolution projection (stepper) lithography of 0.5μm resolution.

CAMB64/POLY-2: Acutely tested 64-channel silicon probes have 63 individual channels arranged in poly-2 style at the edge of the probe with 100 μm site spacing and 21 μm off-set (Figure 1A, also see insert). The top most channel was substituted for an internal reference with surface area = 1404 μm^2 and placed 1.75 mm above the most-proximal site of the probe (not shown). The total cross-sectional area of the individual electrode site was 5,390 μm^2 (Figure 1B). The total coverage of recording electrode sites was 6300 μm. The individual electrode sites were coated with Au and had an impedance of 0.064 ± 0.001 MΩ (mean ± SEM, n_{sites} = 63; n_{probes} = 1). Smaller feature of CAMB64/POLY-2 silicon probes were achieved with a process of high-resolution projection (stepper) lithography of 0.5μm resolution.

The individual electrode sites were coated with various substances. Iridium oxide (IrOx) was used by NeuroNexus to manufacture NN32/TET, NN323/EDGE150, and NN323/EDGE80 silicon probes, platinum (Pt) was used by ATLAS Neuroengineering to manufacture ATLA32/TET silicon probes, and gold (Au) was used by SBM (Scientific & Biomedical Microsystems) and Cambridge NeuroTech to manufacture CAMB64/LIN and CAMB64/PLOY-2 probes.

The available silicon probe technology for large animals suffers from the limitations of low-resolution lithography, which determines the size and spacing of the lines (approximately 4 μm features). It limits the number of sites to plate on standard silicon probe to 32 channels and, therefore, increases the size of the probes which typically have thicknesses of 50-100 μm and widths of 225-250 μm. Currently, 32 individual sites are the upper channel limit with these probes using contact lithography while maintaining reasonable widths. 32-channel silicon probes designed for large animal recordings by ATLAS Neuroengineering (ATLAS32/TET) are 100 μM thick (Figure 1B, yellow), but were silicon the length of the electrode. In contrast, NeuroNexus designed silicone probes are 50 μM thick (NN32/TET, NN32/EDGE150 and NN32/EDGE80) but become brittle beyond 15mm. This necessitated a novel interface cable solution whereby a high density micro-cable is threaded through a 250 μm stainless steel tube and bonded to the contacts at the end of the probe, allowing the probes to be produced in lengths great enough to reach any part of the large

animal brain (Figure 1B; blue, pink, and purple). The CAMB64 design allows for the full length of the hippocampal probe to be manufactured in silicon and in a 64-channel layout (see below).

All multichannel silicon probes used in the study (ATLAS32/TET, CAMB64/LIN, CAMB64/POLY-2, NN32/EDGE150, NN32/EDGE80, and NN32/TET) were custom-designed to have top channel substituted for a low-impedance reference site (surface area of 4200 μm^2) and moved 1-2 mm above the most-proximal probe site (depending on the silicon probe design). Designing the probes with an internal reference for intra-hippocampal recordings may help to reduce noise conferred from the electrical environment by using an electrically inactive but conductive structure such as the CSF of the ventricle in contrast to ECoG style skull screws. We estimated how an introduction of the internal reference affects the noise during awake and anesthetized hippocampal recordings by comparing power of hippocampal oscillation at the level of pyramidal CA1 layer referenced to either an internal or skull screw references (not shown). The internal reference on silicon probes eliminated most of the slow "drift" oscillations as well as 60 Hz frequencies peak, presumably from AC noise during acute recordings, with tether used to record electrophysiological signals. There were no significant differences between either referenced signals during wireless recordings, when FreeLynx used to record/transmit the data (not shown).

Laminar Structure Revealed by Electrode Sites Spacing

The laminar structure of pig dorsal hippocampus was examined electrophysiologically using silicon probes of various designs (Table 1). Laminar structure of the dorsal hippocampus recorded with NN32/EDGE80 silicon probe in an awake behaving pig is shown in Figure 2. The corresponding depths for each layer are: alveus (A) = 173.8 ± 11.55 µm, oriens (O) = 178.3 ± 15.01 µm, pyramidale (P) = 213.2 ±15.9 µm, radiatum (R) = 394.1 ± 22.36 µm, lacunosum-moleculare (L-M) = 223.1 ± 11.7 µm, moleculare (M) = 335.1 ± 17.85 µm, granulosum (G) = 81.3 ± 4.5 µm (see *[18]* for more details). Since the hippocampal region of interest (at our standard recording coordinates in medial-lateral (ML) and anterior-posterior (AP) planes) is about 1600 µm, a silicon probe with 200 µm site spacing will provide good coverage for the laminar structure with enough resolution to identify most layers (Figure 2). We utilized silicon probes with 200 µm (NN32/EDGE150 and NN32/EDGE80, total length = 6200 µm) to examine the whole dorsal hippocampus, including hilus (H), but with this resolution some of the layers could have easily been poorly sampled (such as L-M).

Stability of Neurophysiological Signals Recorded with Silicone Probes over Time

We evaluated the stability of neurophysiological signals recorded from pig hippocampus over time in a sub-sample of these probes. Changes in hippocampal signals were evaluated by using power of LFP signals over time (Figure 3). Since theta (4-10 Hz in pigs) is considered to be a prominent oscillation in pyramidal CA1 layer of hippocampus, we first calculated power of theta (at the stratum radiatum) over the first two weeks post implantation with NN32/EDGE80 silicon probe (Figure 3A). In the first two weeks following surgery,

chronically implanted silicon probes moved slightly, likely due to recovery effects post-surgery such as swelling (Figure 3A). The peak of theta power shifted from channel 8 (Figure 3A, red) to channel 5 (Figure 3A, blue), indicating that NN32/EDGE80 silicon probe moved about 600 µm into the hippocampus (corresponding to a distance between 3 channels on NN32/EDGE probe with 200 µm spacing) as shown in Figure 3Ba. Overall, all previously characterized hippocampal oscillations (low and high gamma, ripple oscillations) decreased over months post-surgery, with the largest drop seen in the first month, potentially due to gliosis/scar tissue formation leading to an insulating/filtering effect on the signal (Figure 3Bb).

In addition to LFPs, we evaluated the amplitude and number of single units recorded in the porcine hippocampus over time (Figure 4). In planar silicon probes, the individual electrode sites were placed on a face of the designs (ATLAS32/TET and NN32/TET). In an attempt to decrease the damage near electrode sites and increase the exposure of the electrode sites to the parenchyma, we designed NN32/EDGE style probe (Figure 1A). In contrast to ATLAS32/TET and NNN32/TET silicon probes, the individual electrode sites on EDGE style probes were strategically positioned on the edge of the substrate, potentially reducing the interference of the insulator with the surrounding signals [28] . Since the 600-6,000 Hz power band representing unit activity decreased over time (Figure 3Bb), we compared the ability of silicone probes to detect single unit activity in the first month post implantation. Single units were recorded in awake behaving pigs for up to three weeks post implantation. Representative single units are shown at one day post-surgery (Figure 4A, D1, see insert). Average amplitude of single units recorded with NN32/EDGE silicon probes was 63 ± 4 µV (n_{cells} = 96) at D1, decreased to 47 ± 6 µV (n_{cells} = 35) at D7 and to 36 ± 2 µV (n_{cells} = 29) at D14. At D21, single units were only detected from NN32/EDGE80 silicon probe, with amplitude of 28 ± 6 µV (n_{cells} = 3) just above a threshold for spike detection (Figure 4A). The number of single units also decreased over the first three weeks, with 64% of single units disappearing by D7 and additional 31% falling below detection threshold by D14 (Figure 4B). NN32/EDGE150 silicon probes had significantly more single units immediately after implantation ($n_{single\ units}$ = 40, pink, $n_{animals}$ = 2) than NN32/EDGE80 ($n_{single\ units}$ = 17, $n_{animals}$ = 1, purple). However, there were no units recorded with NN32/EDGE150 after three weeks, likely due to the tissue damage produced by the wider probe, while NN32/EDGE80 silicon probes still detected single units ($n_{single\ units}$ = 3, $n_{animals}$ = 1, purple). Total number of units averaged over time for combined NN32/EDGE style probes is also shown (Figure 4B, $n_{animals}$ = 3, blue).

Chronic Tissue Response to Implantation of Silicon Probes

We evaluated the tissue response to chronic implantation of 32-channel silicon probes in the hippocampus (Figure 5). Histological examinations performed acutely following electrode insertion (n=3, multiple electrode types within 2-5 hours) demonstrated (as expected) a degree of tissue disruption with associated hemorrhage around the electrode track (Figure 5A). In addition, axonal pathology could be identified immediately adjacent to the site of electrode placement as evidenced by the pathological accumulation of APP, likely

secondary to axonal transection causing acute interruption of transported proteins (Figure 5B). While, direct comparisons of chronic histological outcomes of different electrode types were not performed, preliminary histological evaluations reveal the nature of the pathological response to electrodes in situ over time in swine. Specifically, at 1.5 months post-implantation (n=4, multiple electrode types), hypercellularity was observed surrounding the track. Notably, in one case the choroid plexus could be visualized entering the alveus, presumably having been translocated during the insertion as has previously been visualized (see Figure 8 in [29]) (Figure 5C). Immunostaining revealed both reactive astrocytes, with increased immunoreactivity to GFAP and IBA-1 positive cells with the morphological appearance of reactive microglia (D-F). Interestingly, Van Gieson's staining also revealed collagen surrounding the track (G). Notably, these features were also observed even at 6 months post-implantation, regardless of the type of electrode (n=2) (Figure 5, H-K).

Designing Silicon Probes to Improve Outcome of Chronic Implantation

To improve outcome for future chronic implantations of silicon probes into large animals and to reduce pathological response, novel 64-channel flexible silicon probes CAMB64 were designed and tested acutely. In order to produce longer silicon probes without the need for the extension tube, CAMB64 silicon probes were designed to be manufactured with newer lithography techniques with <1 µm resolution features using a process that allows for stitching across the stepper lithography dies. In order to test stiffness/insertion abilities empirically, mock versions of CAMB64 silicon probes were created to have a fixed width of 80 µm, while the thickness of the mock probes varied in a range of 25-100 µm. The goal was to reduce the profile of the probe, potentially reducing damage to the neural interface and inflammation. Increasing a probe's thickness imparts greater mechanical stiffness of the silicon probe which benefits insertion, but causes a further compliance mismatch between probe and brain tissue, potentially contributing to gliosis and local cell death for chronic implementations. While 25 µm thick mock probes were inserted into cortex, they failed to enter the hippocampal structure, while 35µm and above were capable of insertion into the hippocampus. By reducing the tissue impact during insertion, smaller, more flexible silicon probes may also increase the survival rate of neurons in close proximity to the travel path, but this remains to be determined with chronic implantation. The mock CAMB64 probes were also inserted without support of metal guide tubes, which resulted in less damage to cortical tissue en route to the hippocampus. Based on the insertion ability and acute neuropathology, the 35 µm thick probe was selected for production of initial CAMB64/LIN and CAMB64/POLY-2 silicon probes, giving a minimum dimension for the probes as stiffness increases linearly with width. This novel technology allowed for a doubling of the number of sites on the probe, leading to the first 64-channel probes for large animals that are made exclusively from silicon wafer at lengths capable of reaching much of the large animal brain.

While the linear design is fit for a wide range of applications, isolation of single unit activity may be difficult with only a linear site arrangement. To utilize commercial spike sorting software available at a time (i.e. such as SpikeSort 3D, Neuralynx), individual sites on silicone probes with a linear design were artificially grouped into sets of four (tetrodes)

and then sorted. Single units recorded with 32-channel probes of the earlier designs could not be properly isolated with spike sorting software available at the time, partially due to potential overlap between putative units between the artificial "tetrodes". To address this issue, we initially designed ATLAS32/TET and NN32/TET probe with custom arrangement of electrode sites (Figure 1A). Most of the individual sites were arranged in four sites placed close together (tetrodes), allowing for high-quality cell discrimination in hippocampal recordings, with extra sites in between groups of tetrodes in order to maintain the laminar analyses. Four tetrodes were placed in pyramidal CA1 hippocampal layer (top part of the probe), while three tetrodes were placed in granular cell layer (bottom part of the probe). As tetrode-style silicon probes were created with the individual sites arranged closely to form tetrodes, more single units were isolated but cross-over of the units onto neighboring tetrodes were still observed occasionally in the CA1 layer due to the large size and dendritic arbor of these neurons (not shown).

The advent of laminar spike-sorting software removed the necessity for specific tetrodes to be recreated in the silicon probes, however probe geometry is still an important part of the spike-sorting process [19]. We therefore designed CAMB64 silicon probes with two arrangements of the electrode sites: a linear style CAMB64/LIN probe (148 µm width) and a poly-2 style CAMB64/POLY-2 probe (54 µm width and electrode sites off-set by 21 µm), with tip profile of both probes reduced to a minimum (Figure 1A, see insert). To answer an open question whether non-linear probe designs are necessary for true resolution of single units using modern software such as Klusta/PHY, we compared single-unit separation of a linear vs. a poly-2 CAMB64 silicon probes. Single units were recorded with CAMB 64/LIN and CAMB64/POLY-2 silicon acutely inserted into the same animal. Single units were sorted with PHY software for both designs (Figure 6). Decreasing spacing between individual electrode site to 100 µm on both CAMB64/LIN and CAMB64/POLY-2 style probes helped to sort single units with more precision (Figure 6A). The blue unit on the linear (left) or poly-2 (right) style probes could have easily been classified with the red unit had the spacing not revealed the higher amplitude action potentials at the same time stamps. For single unit separation, the geometry of the poly-2 design appears to better separate single cells compared to the linear design (Figure 6B). Many separated clusters from the CAMB64/LIN recording contained multiple units, which were not well isolated from each other with current spike sorting methods. While some clusters from CAMB64/POLY-2 probe also contained multiple units, the proportion of multi-unit clusters was less when compared to the linear design (33% and 54% respectively). For single units on laminar probes, modern laminar spike sorting methods that classify units based on waveforms across all channels on the probe simultaneously (i.e. Klusta) lead to clusters with poorly defined classic separation measurement thresholds (i.e. L-ratio, Mahalanobis distance) for higher dimensions than tetrodes, but identical criteria were utilized for these electrode comparisons [19, 30].

Discussion

Silicon multichannel probes designed and used for large animal hippocampal electrophysiology allow for a longer area of coverage in contrast to single site recordings with tungsten electrodes, as well as revealing laminar structure and correlation of unit activity with field behavior. We have performed a retrospective analysis of acute and chronically implanted pigs from our experiments in order to characterize the differences in electrophysiology over time with various probe sizes and geometries from different manufacturers. In addition, we have examined the neural interface out to 6 months post-implantation in order to assess whether neuropathology in the large animal hippocampus resembles that previously reported in rodents. Differing probe geometries were examined in a new higher density research probe in order to assess their ability for sorting units. Long-length silicon probes may also replace the need for multiple insertion acute experiments if the animal is chronically implanted and/or a drive is utilized.

Our initial attempts at chronic implantations using probes that were developed for acute work and prior to modern spike sorting methods for laminar probes were successful only for field recordings. Units that appeared during implantation surgery were not present or significantly attenuated even 24 hours post implantation. Histological examination suggested that the damage to the neural interface, and sometimes the cytoarchitecture, was significant with these larger dimension probes. In addition, attenuation of units over time as well as field data in various frequency ranges is potentially explained by both cellular and collagen encapsulation of the probe as demonstrated at 6 weeks and 6 months post implantation. We therefore redesigned these probes to increase laminar coverage, as well as placing the electrodes on the edge of the probe in order to take full advantage of the contacts as has previously been described [28]. This change in dimension and geometry had the effect of increasing unit yields for the initial two to three weeks post implantation, with significant attenuation by the third week. Further reduction of the width by almost a factor of two at the top of active portion of the probe yielded a greater number of units in one animal at week three, but needs to be replicated to draw any conclusions regarding this final width change. It is an open question how much the placement of the edge electrodes increased unit longevity in relationship to the width change, but newer designs with offset spacing may allow for future examination of this relationship that has previously been reported. Further detailed quantification of the differences in chronic neuropathology with various probe dimensions is also warranted to examine the potential correlation between these improved results and differences in the chronic neural interface response.

We also tested various designs of silicon probes available from and developed with the manufacturers for the ability to separate single units. Linear, tetrode plus linear and poly-2 designs arrangement design were evaluated for single unit vs. multi-unit cluster isolation. Spacing between individual electrode sites played a significant role as 200 μm spacing (as on NN32/EDGE style probes) increased the number of multi-units sorted. This could affect the precision of research studies focused on activity of hippocampal neurons, for example characterization of place cells or interneurons. Interestingly, some CA1 units spanned not

two, but three electrodes, suggesting that large putative pyramidal cells that run parallel to the probe can be detected across greater distances than those previously reported, and further suggesting that lateral electrode separation for analysis in these structures may be helpful. Although most of the probes with a linear design site arrangement (NN32/EDGE150, NN32/EDGE80, and CAMB64/LIN) were able to record neuronal activity of individual neurons, silicon probes with a tetrode (ATLAS32/TET and NN32/TET) and a poly-2 (CAMB64/POLY-2) design site arrangement had better cluster separation with currently available sorting algorithms, as the proportion of single units to multi-units recorded with a given probe increased. Previous acute examinations in large animals have also noted the usefulness of the parallel geometry in isolating units, even prior to the advent of new sorting techniques [13]. New sorting techniques, as well as drift associated with the semi-floating chronic preparation, suggest that parallel configurations may be optimal in order to maximize unit detection and separation in large animal laminar structures, and may be helpful as drives are developed for these probes.

Mock probe testing of the CAMB64 25mm-long probes demonstrated that 35 µm shank thickness for 80 µm wide probes strikes an ideal compromise between ease of tissue penetration and appropriate targeting vs. the need to maintain small device dimensions. This allowed for production and testing of the 30 mm long 64-channel probes described above, which yielded substantially more units in the poly-2 style probe in acute testing. The balance between maximal stiffness, length and electrode density with minimal cross-sectional area in order to reduce damage to the neural interface remains a significant challenge in large animals. Designs such as the NeuroNexus' NN32/EDGE probe and the new CAMB64 probe approach these challenges with different design solutions, but appear to have reached a critical threshold where the full depth can be reached with enough electrodes for sorting, and allowing for single unit detection out to a month post implant without being driven. Future chronic implantation of the CAMB64 electrodes will further test whether the trade-off of device width for increased channel count increases single unit yield, and for how long. These probes are also not at the minimal feature dimensions for this technique, as electrode yield in the initial testing run was also a consideration. Future dimensions of 80µm wide, 64-channel probes may also increase yield by reducing damage to the neural interface, but this remains to be tested as well.

Conclusions

We hope that this study will help to facilitate development of novel silicon multi-channel probes suitable for chronic implantations in large animals, by comparing silicon probes available for use in large animal electrophysiology, as well as comparing them to a new design and process. NeuroNexus EDGE style probes (NN32/EDGE80) were determined to yield the largest number of units of the available probes for acute and chronic recordings from laminar structures due a linear edge site arrangement, 6mm of coverage, and potentially reducing damage to the neural interface upon insertion. In addition, cross-sectional area was found to be one determinant of silicon probes' performance. Novel CAMB64 silicon probes

with a poly-2 design were found to have an even better single unit separation and a denser sampling of the laminar structure than existing linear probes. By increasing channel density, we were able to better visualize laminar structure and create offset geometries that enabled better unit sorting, however it is an open question what the optimal channel density is for this structure and requires chronic implantation. Channel density, site arrangement, and physical profile of the silicon probe are all important factors to consider when designing probes for acute and chronic implantations to study laminar structures over time in awake behaving animals. We hope these results will lower the threshold for adoption in chronic implantations, by demonstrating consistent yields in laminar electrophysiological recordings in large animals using commercially available probes. We hope that in combination with new wireless technologies allowing for freely moving behavior, this will support new discoveries in both hippocampal and neocortical neurophysiology. In addition, better detection and understanding of laminar circuitry and changes in human disease (i.e. epilepsy, traumatic brain injury) are needed, and therefore viable electrodes need to be tested first in translational large animal models prior to clinical use.

Author Contributions: Conceptualization, A.U. and J.W.; Methodology, A.U., P.K., T.H., B.J., and J.W.; Software, A.U., C.A., P.K, and J.W.; Validation, A.U., C.A., P.K, H.I.C., V.J., J.W.; Formal Analysis, A.U., C.A., C.C., K.G.; Investigation, A.U., C.A., P.K., K.G., J.W.; Resources, D.K.C. and J.W.; Data Curation, A.U.; Writing-Original Draft Preparation, A.U.; Writing-Review & Editing, A.U., C.A., K.G. and J.W.; Visualization, A.U. and J.W.; Supervision, J.W.; Project Administration, J.W.; Funding Acquisition, J.W.

Funding: This research was funded by the Department of Veterans Affairs, grant numbers IK2-RX001479 and I01-RX001097, the National Institutes of Health, grant numbers NINDS R01-NS-101108-01 and T32-NS043126, CURE Foundation, Taking Flight Award, and DoD ERP CDMRP, grant number W81XWH-16-1-0675, and W81XWH-15-9-0001.

Acknowledgments: Authors would like to thank Adolf Dossman, Michael R. Grovola, Matthew Sergison, and Maura T. Weber for their help with the experimental design and execution.

Conflicts of Interest: The authors declare no conflict of interest. The founding sponsors had no role in the design of the study; in the collection, analyses, or interpretation of data; in the writing of the manuscript, and in the decision to publish the results.

References

1. Bragin, A., et al., *Gamma (40-100 Hz) oscillation in the hippocampus of the behaving rat.* The Journal of Neuroscience, 1995. **15**(1): p. 47.
2. Bragin, A., et al., *Dentate EEG spikes and associated interneuronal population bursts in the hippocampal hilar region of the rat.* Journal of Neurophysiology, 1995. **73**(4): p. 1691.
3. Buzsáki, G., *Two-stage model of memory trace formation: A role for "noisy" brain states.* Neuroscience, 1989. **31**(3): p. 551-570.
4. Buzsáki, G., *Hippocampal sharp wave-ripple: A cognitive biomarker for episodic memory and planning.* Hippocampus, 2015. **25**(10): p. 1073-1188.
5. Buzsáki, G., et al., *Hippocampal network patterns of activity in the mouse.* Neuroscience, 2003. **116**(1): p. 201-211.
6. Lewis, C.M., C.A. Bosman, and P. Fries, *Recording of brain activity across spatial scales.* Current opinion in neurobiology, 2015. **32**: p. 68-77.
7. Stevenson, I.H. and K.P. Kording, *How advances in neural recording affect data analysis.* Nature Neuroscience, 2011. **14**: p. 139.
8. Vetter, R.J., et al., *Chronic neural recording using silicon-substrate microelectrode arrays implanted in cerebral cortex.* IEEE Transactions on Biomedical Engineering, 2004. **51**(6): p. 896-904.
9. Fernández-Ruiz, A., et al., *Entorhinal-CA3 Dual-Input Control of Spike Timing in the Hippocampus by Theta-Gamma Coupling.* Neuron, 2017. **93**(5): p. 1213-1226.e5.
10. Hainmueller, T. and M. Bartos, *Parallel emergence of stable and dynamic memory engrams in the hippocampus.* Nature, 2018. **558**(7709): p. 292-296.
11. Kee, S.E., et al., *Impaired spatial memory codes in a mouse model of Rett syndrome.* eLife, 2018. **7**: p. e31451.
12. Killian, N.J., M.J. Jutras, and E.A. Buffalo, *A map of visual space in the primate entorhinal cortex.* Nature, 2012. **491**: p. 761.
13. Blanche, T.J., et al., *Polytrodes: High-Density Silicon Electrode Arrays for Large-Scale Multiunit Recording.* Journal of Neurophysiology, 2005. **93**(5): p. 2987-3000.
14. Buzsáki, G., *Large-scale recording of neuronal ensembles.* Nature Neuroscience, 2004. **7**: p. 446.
15. Duhaime, A.-C., et al., *Maturation-dependent response of the piglet brain to scaled cortical impact.* Journal of Neurosurgery, 2000. **93**(3): p. 455-462.
16. Flynn, T., *Developmental changes of myelin-related lipids in brain of miniature swine.* Neurochem Res, 1984. **9**(7): p. 935-45.
17. Pampiglione, G., *Some aspects of development of cerebral function in mammals.* Proceedings of the Royal Society of Medicine, 1971. **64**(4): p. 429-435.
18. Ulyanova, A.V., et al., *Electrophysiological Signature Reveals Laminar Structure of the Porcine Hippocampus.* bioRxiv, 2017.
19. Rossant, C., et al., *Spike sorting for large, dense electrode arrays.* Nat Neurosci, 2016. **19**(4): p. 634-641.

20. Mitra, P.P.B., Hemant, *Observed brain dynamics*. 1 edition ed. 2007: Oxford University Press. 408.
21. Hazan, L., M. Zugaro, and G. Buzsáki, *Klusters, NeuroScope, NDManager: A free software suite for neurophysiological data processing and visualization.* Journal of Neuroscience Methods, 2006. **155**(2): p. 207-216.
22. Johnson, V.E., et al., *SNTF immunostaining reveals previously undetected axonal pathology in traumatic brain injury.* Acta Neuropathologica, 2016. **131**(1): p. 115-135.
23. Johnson, V.E., et al., *Mechanical disruption of the blood–brain barrier following experimental concussion.* Acta Neuropathologica, 2018. **135**(5): p. 711-726.
24. Johnson, V.E., et al., *SNTF immunostaining reveals previously undetected axonal pathology in traumatic brain injury.* Acta Neuropathol, 2016. **131**(1): p. 115-35.
25. Johnson, V.E., et al., *Mechanical disruption of the blood-brain barrier following experimental concussion.* Acta Neuropathol, 2018. **135**(5): p. 711-726.
26. Johnson, V.E., et al., *Inflammation and white matter degeneration persist for years after a single traumatic brain injury.* Brain, 2013. **136**(1): p. 28-42.
27. Maas, A.I.R., et al., *Traumatic brain injury: integrated approaches to improve prevention, clinical care, and research.* The Lancet Neurology, 2017. **16**(12): p. 987-1048.
28. Lee, H.C., et al., *Placing Sites on the Edge of Planar Silicon Microelectrodes Enhances Chronic Recording Functionality.* IEEE Transactions on Biomedical Engineering, 2018. **65**(6): p. 1245-1255.
29. Skaggs, W.E., et al., *EEG Sharp Waves and Sparse Ensemble Unit Activity in the Macaque Hippocampus.* Journal of Neurophysiology, 2007. **98**(2): p. 898-910.
30. Schmitzer-Torbert, N., et al., *Quantitative measures of cluster quality for use in extracellular recordings.* Neuroscience, 2005. **131**(1): p. 1-11.

Figure 1. Design of multichannel silicon probes used for acute and chronic hippocampal recordings in pigs. A) The arrangement of the individual electrode sites is shown for 32-channel silicon probes ATLAS32/TET (yellow), NN32/TET (blue), NN32/EDGE150 (pink), and NN32/EDGE80 (purple). 64-channel silicon probes CAMB64/LIN and CAMB64/POLY-2 were also tested acutely (orange). The arrangement of electrode sites for CAMB64/LIN and CAMB64/POLY-2 is shown magnified in the insert (bottom panel). Cross-sectional area at the top electrode site is shown at the top. All silicon probes had an internal reference placed 1-2 mm above the most-proximal electrode site (not shown). **B)** Comparison of width and thickness of silicon probes is shown overlaid on each other (colors are the same as in A). The corresponding widths are 215 µm for ATLAS32/TET (yellow), 150 µm for NN32/EDGE150 (pink), 80 µm for NN32/EDGE80 (purple), 225 µm for NN32/TET (blue), and 151 µm for CAMB64/LIN/POLY-2 (orange) silicon probes. NN32/EDGE150 is shown as a continuation of NN32/EDGE80. The thickness of silicon probes is 100 µm for ATLAS32/TET, 50 µm for NN32/EDGE150, NN32/EDGE80, NN32/TET, and 35 µm for both CAMB64/LIN and CAMB64/POLY-2 probes (orange).

Figure 2. Chronic hippocampal recordings in awake behaving pigs. Recording with NN32/EDGE silicon probe with a linear arrangement of electrode sites (200 µm site spacing) was done in the awake behaving animal. The silicon probe was placed in the dorsal hippocampus so that it covers hippocampal layers of stratum oriens (O), pyramidale (P), radiatum (R), lacunosum-moleculare (L-M), moleculare (M), granulosum (G), and hilus (H). A representative hippocampal section stained with LFB/CV is overlaid on laminar oscillatory activity to match representative layers as described previously [18]. A single ripple event can be seen in CA1 layer (arrow).

Figure 3. Power of main hippocampal oscillations decreases over months following chronic implantation. A) Over a period of two weeks, chronically implanted NN/EDGE80 silicon probe moved deeper into the dorsal hippocampus. One day post- implant, theta oscillation (5-10 Hz) was maximum at channel 8 (blue trace). Over the course of two weeks, the theta peak moved up 3 electrode sites (red trace). The grey dotted line indicates the pyramidal CA1 layer. **Ba)** The silicon probe's drift was calculated for NN/EDGE80 silicon probe as a drift of theta power, which peaks in stratum-radiatum (blue trace). NN/EDGE80 probe moved down into the dorsal hippocampus for 600 µm in a course of 12 days following chronic implantation surgery. **Bb)** Overall power of hippocampal oscillations (θ (5-10 Hz), γ_{low} (25-55 Hz), γ_{high} (60-110 Hz), ρ (110-200 Hz), and (600-6,000 Hz)) in porcine dorsal hippocampus decreased over months, with significant drop in the first month. The total power is shown with a dotted line.

Figure 4. Single units recorded for three weeks post implantation. A) Single units were recorded in awake behaving pigs for up to three weeks post implantation (n = 3). Representative single units are shown (at D1, see insert). The amplitude of single units decreased over time and reached threshold for detection (above 35 µV) at D21. At this point, only NN32/EDGE80 silicon probe had single units recorded (3 single units, D21). **B)** An

ability to detect single unit activity was compared for NN32/EDGE150 and NN32/EDGE80 over three weeks period. NN32/EDGE150 silicon probes ($n_{single\ units} = 40$, pink, $n_{animals} = 2$) had significantly more single units immediately after implantation (D1) than NN32/EDGE80 ($n_{single\ units} = 17$, $n_{animals} = 1$, purple). However, there were no units recorded with NN32/EDGE150 after three weeks (D21), while NN32/EDGE80 silicon probes still detected single units ($n_{single\ units} = 3$, $n_{animals} = 1$, purple). Total number of units averaged over time for combined NN32/EDGE style probes is also shown ($n_{animals} = 3$, blue).

Figure 5. Acute and chronic response to implantation of silicon probes in large animals. **(A)** H&E staining showing electrode track with associated hemorrhage acutely (<5h) following insertion of NN32/TET electrode. **(B)** APP immunohistochemistry showing the same region as (A). Note the axonal swellings indicative of axonal transport interruption, likely secondary to axonal transection during insertion. Surrounding pyramidal neurons also show increased APP immunoreactivity**. (C)** Van Gieson stain showing electrode track 1.5 months following implantation of NN32/EDGE80 electrode where collagen is pink. Notably, there appears to be choroid plexus abnormally located within the alveus. **(D-G)** Neuropathological findings in NN32/TET electrode track, 1.5 months following implantation, demonstrating (**D**) lesion with (**E**) IBA-1 positive cells displaying morphological features of activated microglia, **(F)** GFAP immunoreactive cells with features of reactive astrocytes and **(G)** Van Gieson staining demonstrating the presence of collagen (pink). **(H-K)** Electrode track 6 months following implantation of NN32/TET, again showing surrounding activation of both microglia **(I)** and astrocytes **(J)**, as well as the presence of collagen **(K)**. Scale bars: A, B, D-K:100µm; C: 200µm.

Figure 6. Novel research CAMB64 silicon probes tested acutely neurophysiological responses after insertion into the porcine hippocampus. A) Single units were isolated for a linear and a poly-2 designs CAMB64 silicon probes. Decreasing spacing between individual electrode site to 100 µm on both CAMB64/LIN and CAMB64/POLY-2 style probes helped to sort single units with more precision. The blue unit on the linear (left) or poly-2 (right) style probes could have easily been classified with the red unit had the spacing not revealed the higher amplitude action potentials at the same time stamps. **B)** Spike sorting on a recording with CAMB64/LIN silicon probe yielded more multi-units (red, n = 20) than single units (green, n = 17). While some clusters on CAMB64/POLY-2 silicon probe contained multiple units (red, n = 24), two times more single units (green, n = 48) were identified. Also, the proportion of multi-unit clusters for poly-2 design was less when compared to the linear design (33% and 54% respectively).

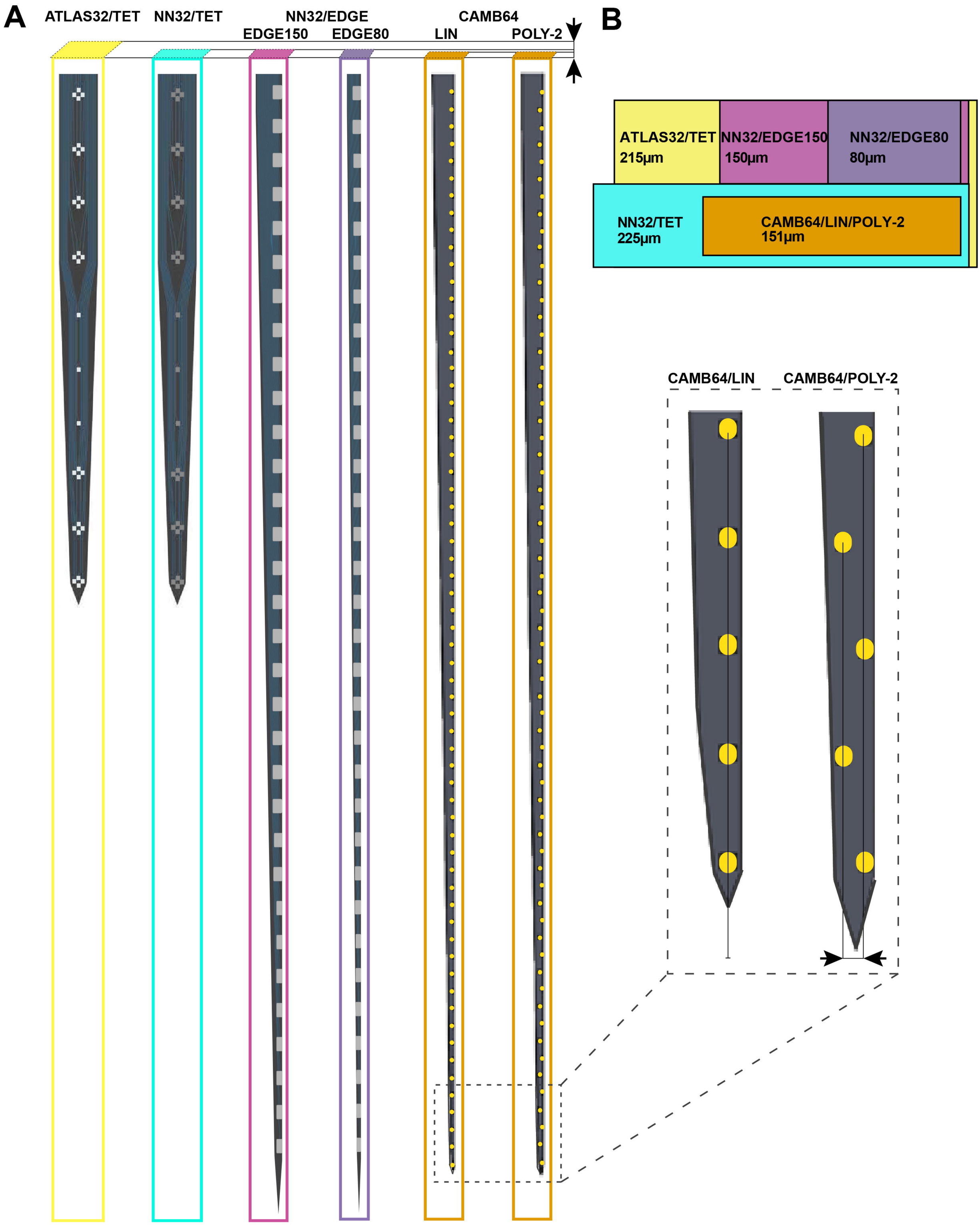
A
ATLAS32/TET
NN32/TET
NN32/EDGE
EDGE150
EDGE80
CAMB64
LIN
POLY-2
B
ATLAS32/TET
215µm
NN32/EDGE150
150µm
NN32/EDGE80
80µm
NN32/TET
225µm
CAMB64/LIN/POLY-2
151µm
CAMB64/LIN
CAMB64/POLY-2

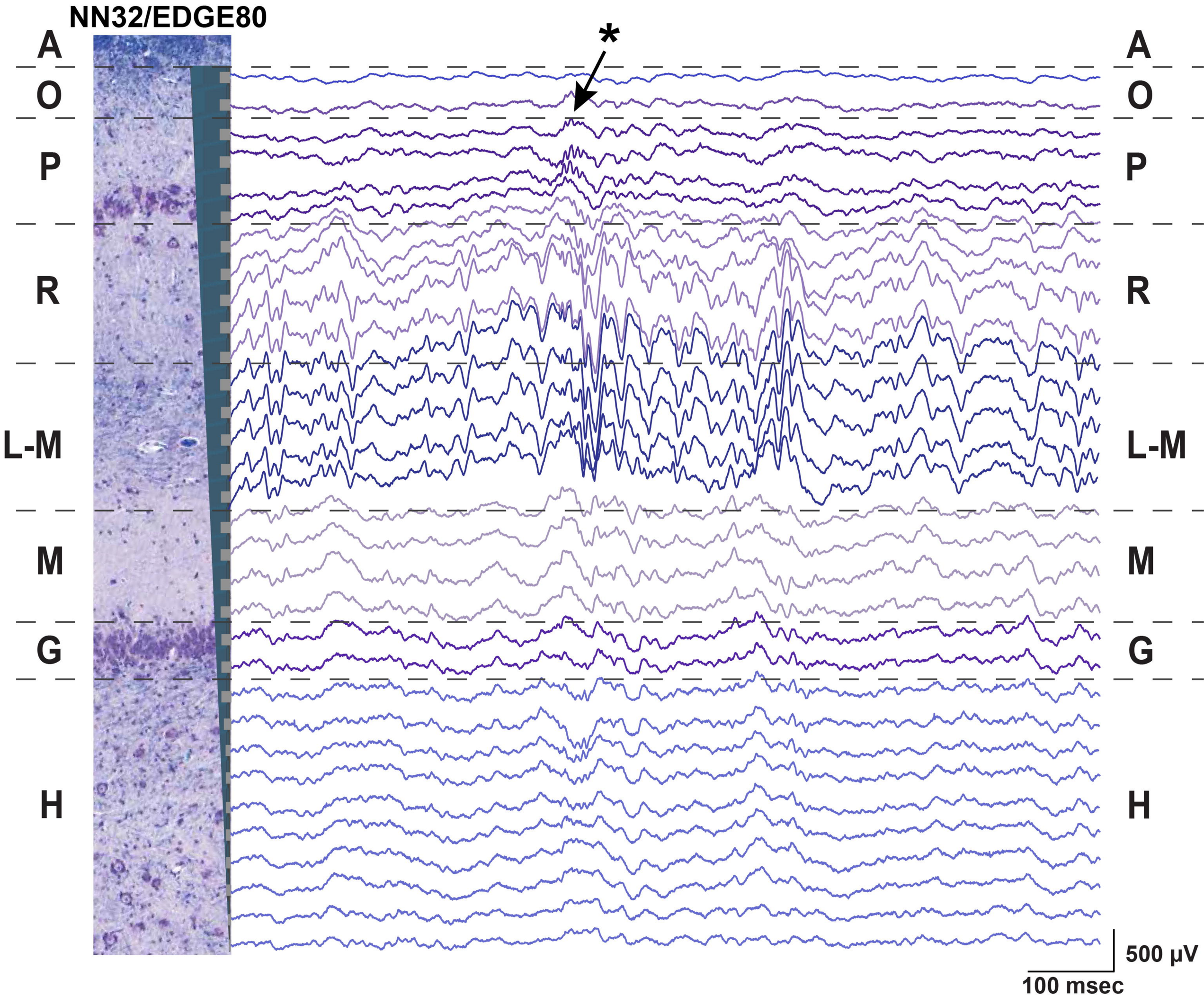
NN32/EDGE80
A
O
P
R
L-M
M
G
H
*
500 µV
100 msec

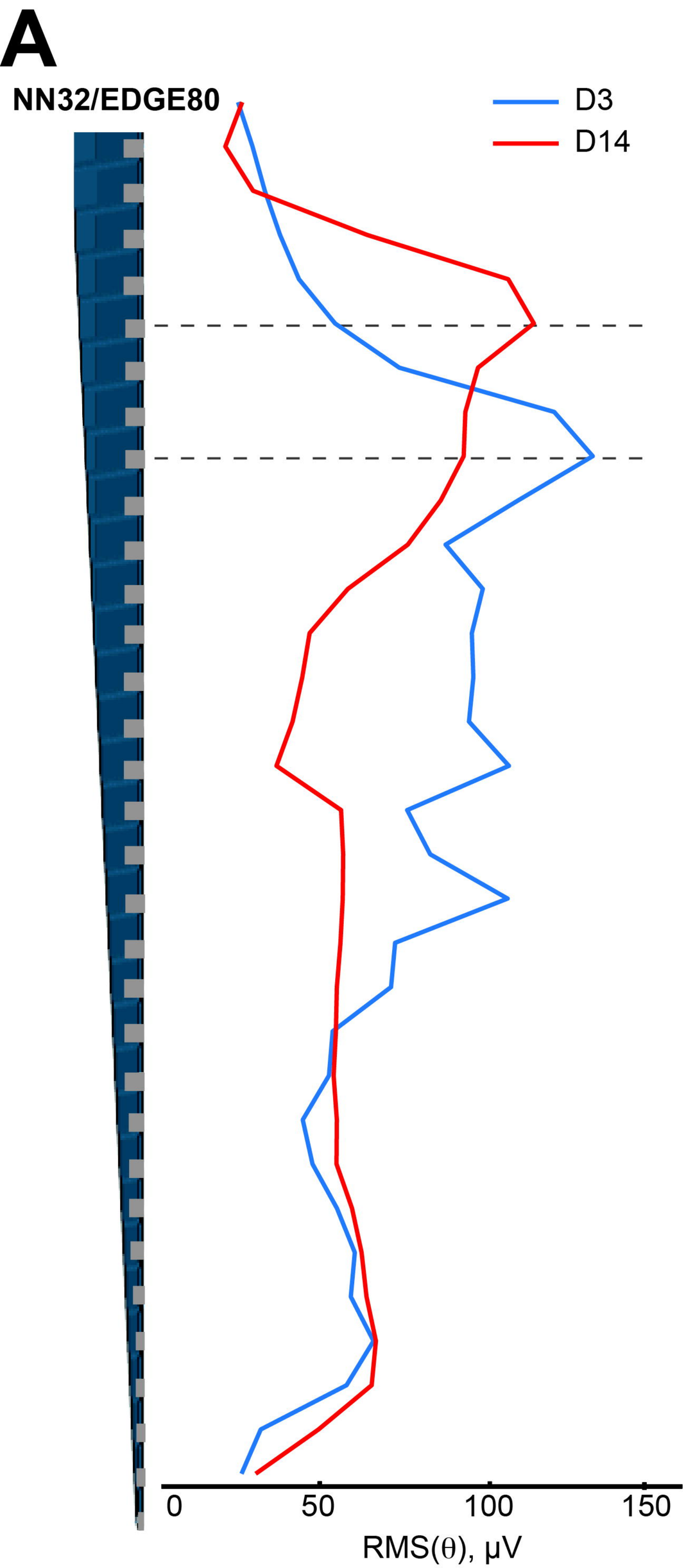
A
NN32/EDGE80
D3
D14
0
50
100
150
RMS(θ), μV

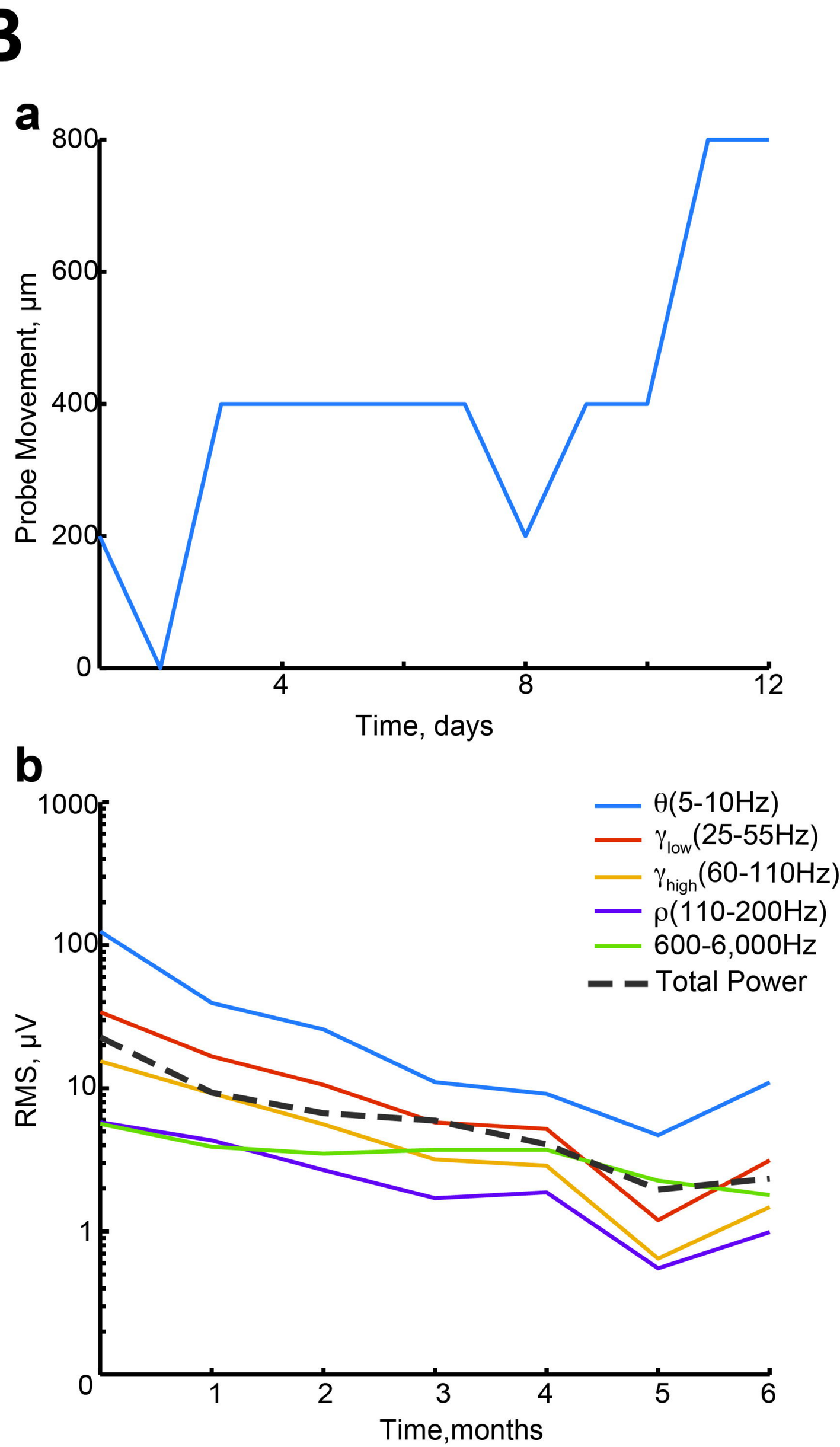
B
a
800
600
400
200
0
Probe Movement, μm
4
8
12
Time, days
b
1000
100
10
1
0
RMS, μV
θ(5-10Hz)
γlow(25-55Hz)
γhigh(60-110Hz)
ρ(110-200Hz)
600-6,000Hz
Total Power
1
2
3
4
5
6
Time,months

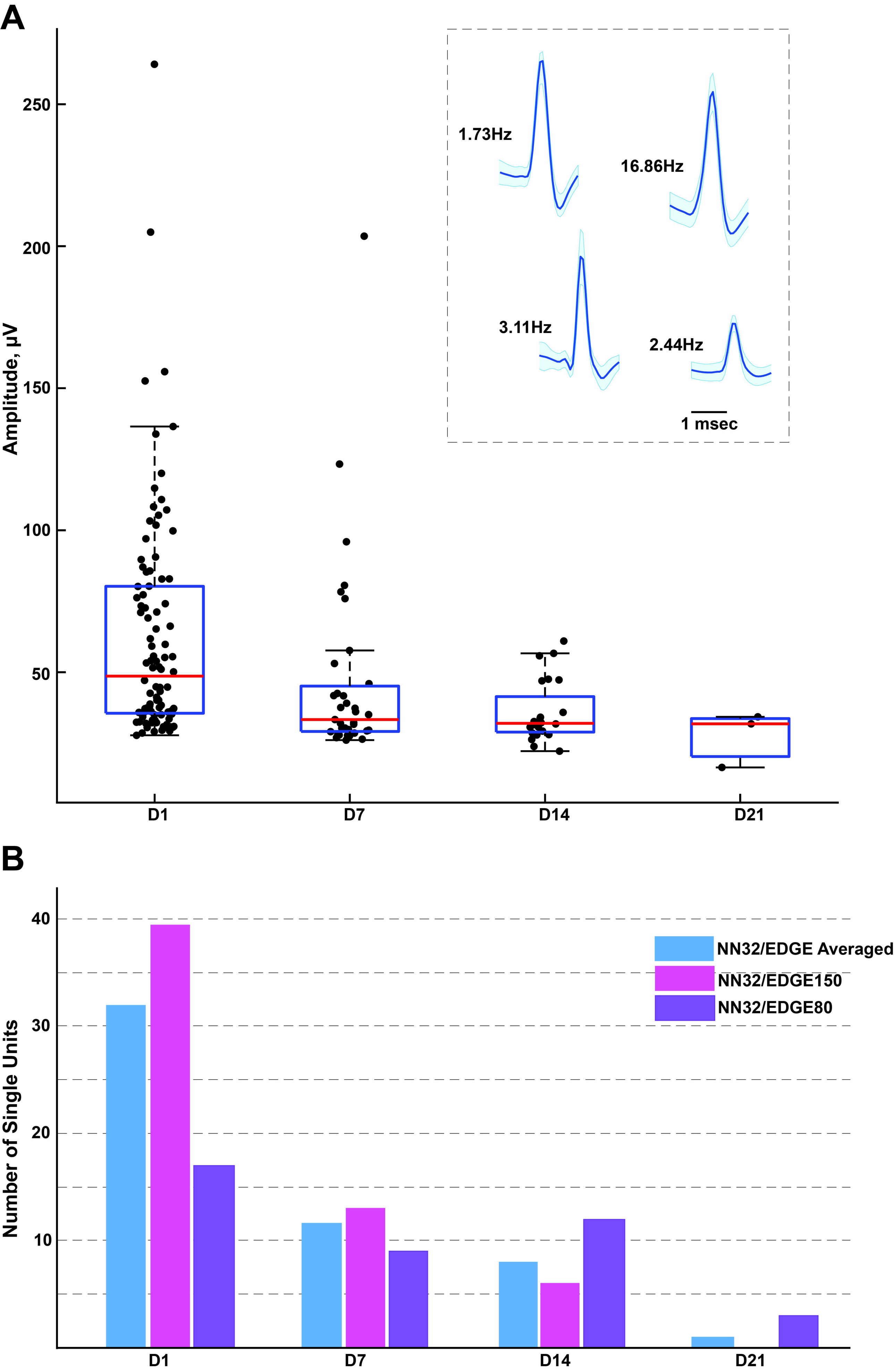
A
Amplitude, µV
250
200
150
100
50
D1
D7
D14
D21
1.73Hz
16.86Hz
3.11Hz
2.44Hz
1 msec
B
Number of Single Units
40
30
20
10
NN32/EDGE Averaged
NN32/EDGE150
NN32/EDGE80
D1
D7
D14
D21

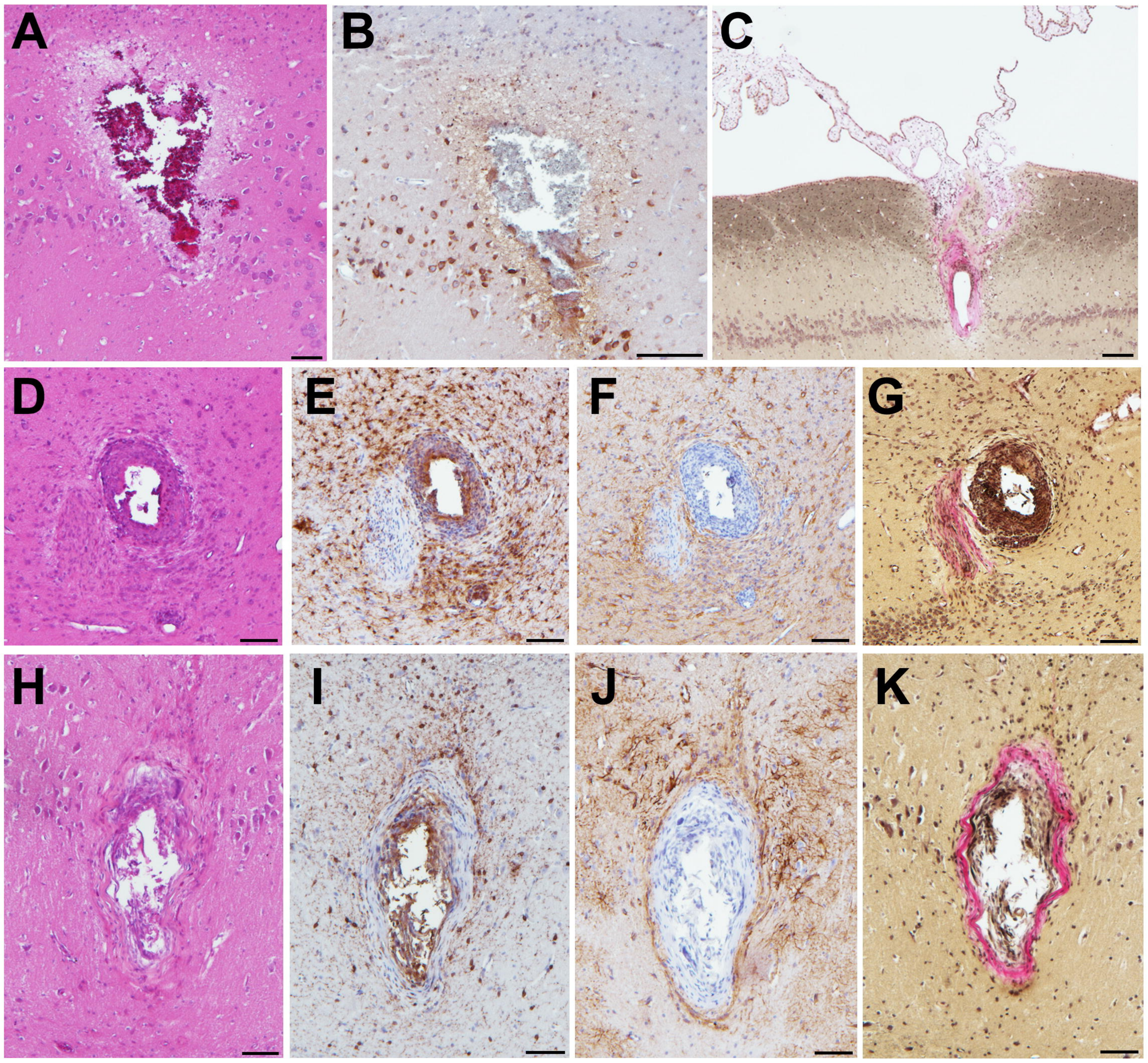
A
B
C
D
E
F
G
H
I
J
K

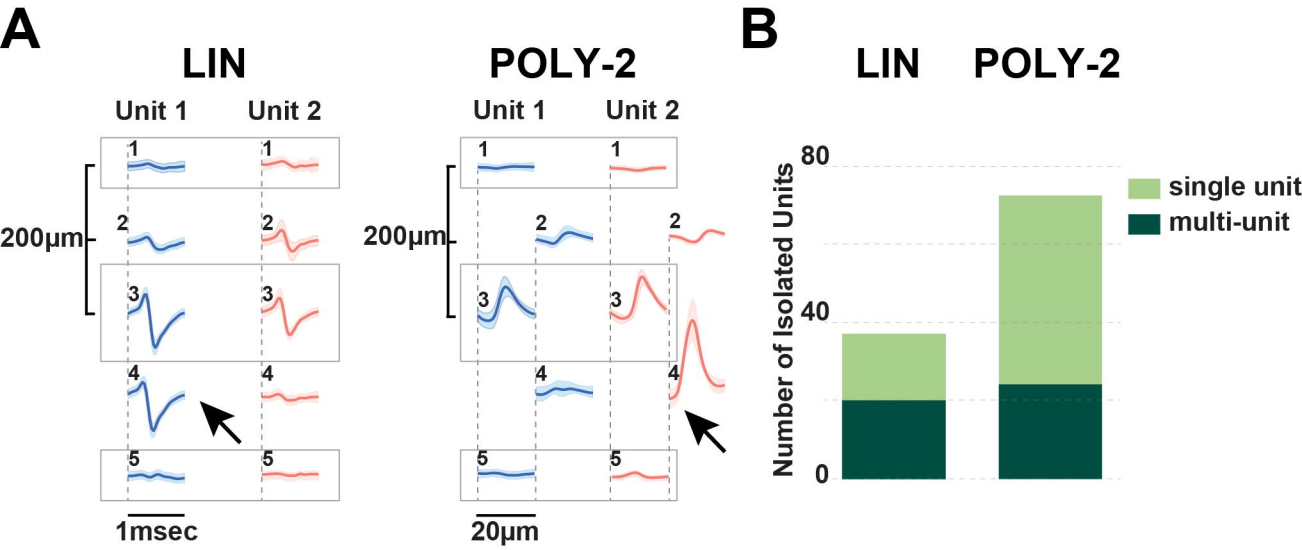
A
LIN
POLY-2
Unit 1
Unit 2
Unit 1
Unit 2
200µm
200µm
1
2
3
4
5
1msec
20µm
B
LIN
POLY-2
Number of Isolated Units
80
40
0
single unit
multi-unit